Journal of Innovative Optical Health Sciences
Vol. 8, No. 5 (2015) 1550041 (8 pages)

DOI: 10.1142/S1793545815500418

World Scientific
www.worldscientific.com



# Hidden stage of intracranial hemorrhage in newborn rats studied with laser speckle contrast imaging and wavelets

Alexey N. Pavlov*, Arkady S. Abdurashitov, Olga N. Pavlova and Valery V. Tuchin
*Department of Physics, Saratov State University*
*83 Astrakhanskaya Str., Saratov 410012, Russia*
**pavlov.lesha@gmail.com*

Olga S. Sindeeva, Sergey S. Sindeev and Oxana V. Semyachkina-Glushkovskaya†
*Department of Biology, Saratov State University*
*83 Astrakhanskaya Str., Saratov 410012, Russia*
†*glushkovskaya@mail.ru*

Received 15 March 2015
Accepted 3 May 2015
Published 12 June 2015

Using the laser speckle contrast imaging and wavelet-based analyses, we investigate a latent (a "hidden") stage of the development of intracranial hemorrhages (ICHs) in newborn rats. We apply two measures based on the continuous wavelet-transform of blood flow velocity in the sagittal sinus, namely, the spectral energy in distinct frequency ranges and a multiscality degree characterizing complexity of experimental data. We show that the wavelet-based multifractal formalism reveals changes in the cerebrovascular blood flow at the development of ICH.

*Keywords*: Cerebral blood flow; laser speckle contrast imaging; stress; wavelet-analysis; complexity.

## 1. Introduction

Despite the intracranial hemorrhage (ICH) is related to main reasons of neonatal morbidity and mortality,[1,2] mechanisms responsible for its development are still poorly understood. This development is typically asymptomatic, and a latent period of the transformation of normal physiological processes into pathological dynamics can easily be overlooked. Due to this circumstance, effective markers of the hidden stage of the ICH development are of high importance. ICH typically occurs at the second day after birth. Aiming to reveal a high risk for this pathology, analysis of impairments of the cerebral venous blood flow (CVBF) should be performed during several hours after birth.[3,4] Besides noninvasive experimental techniques, this analysis

*Corresponding author.

requires processing of quite short and nonstationary data reflecting the cerebrovascular dynamics.

A widely used noninvasive technique for measuring CVBF is the laser speckle contrast imaging (LSCI)[5–7] that possesses a high spatio-temporal resolution. Dynamics of CVBF is characterized based on variations of the speckle pattern that is formed due to the scattering of the coherent light from moving particles in blood. Temporal changes of the contrast quantify the velocity of blood flow. During the last decades, the LSCI technique was widely applied in solving various medical problems providing a way to analyze the blood perfusion in retina, skin and other tissues.

An effective approach for extracting information from short, noisy and nonstationary data is the wavelet-analysis[8–12] that has demonstrated its essential potential in different areas of natural sciences. Wavelet-based methods often outperform the standard data processing tools such as, e.g., the spectral or the correlation analysis. Thus, analysis of long-range correlations with wavelets can be done using significantly shorter time series as compared with the correlation function.[13,14] Characterizing adaptation processes in the cardiovascular system with wavelets allows revealing distinct stress-induced responses that are not distinguished with the spectral analysis.[15] Besides, wavelet-based tools provide additional information about interactions of physiological control mechanisms.[16,17]

In this paper, we study the abilities of wavelet-based diagnostics of impairments in the cerebral blood flow that occur during the hidden stage of the ICH development. The paper is organized as follows. In Sec. 2, we describe the experimental techniques and methods used for data processing. Analysis of the latent stage of stress-induced ICH development in newborn rats and a discussion of markers that can be applied for early diagnostics are given in Sec. 3. Section 4 contains some concluding remarks.

## 2. Experiments and Data Processing

### 2.1. *Subjects*

Experiments were performed in 59 newborn male rats (2–3 days after birth) in accordance with the Guide for the Care and Use of Laboratory Animals (NIH Publication No. 85-23, revised 1996). Protocols were approved by the Committee for the Care and Use of Laboratory Animals at Saratov State University (Saratov, Russia). Animals were housed at $25 \pm 2^{\circ}$C, 55% humidity and 12:12 h light/dark cycle.

A previously described model of a severe stress[18,19] was applied to induce the ICH in newborn rats. The animals were placed in the Plexiglas chamber (volume — 2000 cm$^3$) and underwent intermittent infra-sound (10 Hz, 120 dB) that repeated during 2 h (10 s — the sound, 60 s — the interruption). The appearance of ICH during the next day after such stress was verified by magnetic resonance imaging and histological studies.[18]

Three groups of newborn rats were selected for further analysis of CVBF: a control group (unstressed rats, $n = 19$), stressed rats with the hidden stage of ICH (4 h after the stress-off, $n = 18$), and stressed rats with ICH (24 h after the stress-off, $n = 22$).

### 2.2. *Laser speckle contrast imaging*

LSCI was used to measure CVBF through the fontanel in anesthetized rats (isoflurane — inhalant anesthetic) with the fixed head. This optical technique allows monitoring of cerebral blood flow in selected vessels.[5–7,20] Laser speckle is a pattern obtained due to the scattering of coherent light from analyzed object. In case of rough surfaces, the light intensity at the chosen point depends on the differences of the optical path for the reflected waves. For large differences compared with the light wavelength, essential variations of the intensity occur; it reduces for anti-phase waves and increases for in-phase waves. Due to the presence of scattering particles in blood moving through the vessel, the intensity demonstrates a temporal variation that is used to analyze dynamical changes in cerebrovascular dynamics.

In this study, blood flow in the sagittal sinus was analyzed. Speckle images were acquired with the following set up: the exposed rat cortex was illuminated by the HeNe laser (Thorlabs HNL210L, 632.8 nm) coupled with the single mode fiber (Thorlabs PMC630-50B-APC). Raw laser speckle images (Fig. 1) were recorded using monochromatic CMOS camera Basler acA2500-14 gm and Computar M1614-MP2 lens in which F-number was adjusted to meet the Nyquist criterion[21] (two pixels per speckle). Speckle images were acquired at the rate of 40 frames/second during 5 min. Aiming to

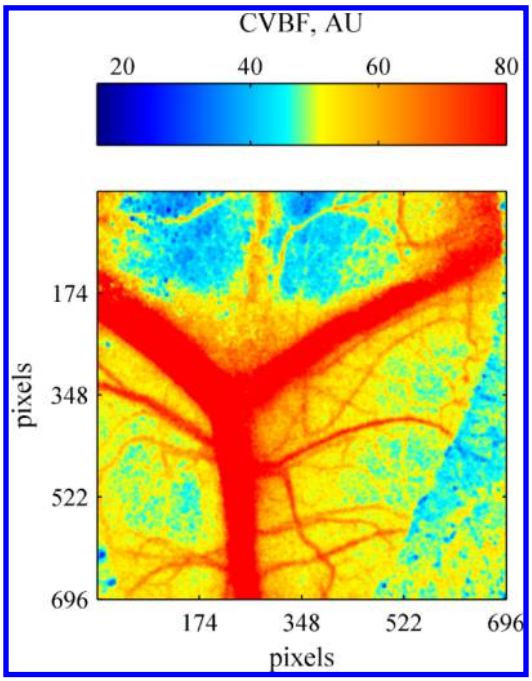


Fig. 1. An example of speckle contrast image of the superior sagittal sinus perfusion.

reduce noise in raw images, data preprocessing was performed consisting of time averaging over 50 images using a moving window (55 × 55 pixels). We applied here the Gaussian approach to convert the speckle contrast data into flow velocity data being more suitable for ordered flows. Dynamical changes of CVBF characterizing the macroscopic cerebral dynamics were recorded. A single data series of the blood flow velocity in the sagittal sinus was analyzed for each animal.

### 2.3. *Scalograms*

CVBF dynamics was studied with the wavelet-based spectral analysis.[10,11] Unlike the standard spectral analysis based on the windowed Fourier transform, application of wavelets has an advantage for short data providing smoother dependencies of the spectral energy vs the frequency of oscillations (the scalograms).

The continuous wavelet-transform of blood flow velocity was performed as follows

$$W(a,b) = \frac{1}{\sqrt{a}} \int_{-\infty}^{\infty} x(t)\psi^*\left(\frac{t-b}{a}\right)dt, \qquad (1)$$

where $W(a,b)$ are the wavelet transform coefficients, $a$ and $b$ are the scale and the translation parameters, respectively, and $\psi$ is the basic wavelet. When performing spectral analysis, complex-valued wavelets are typically applied with the Morlet wavelet representing the most popular wavelet-function

$$\psi(\tau) = \frac{1}{\pi^{0.25}} \exp(j2\pi f_0\tau) \exp\left(-\frac{\tau^2}{2}\right), \qquad (2)$$

where the parameter $f_0$ is the central frequency that determines the number of oscillations. For $f_0 = 1$, there is a simple relation between the scale $a$ and the Fourier-frequency $f$, namely, $f = 1/a$. Further we shall consider frequencies instead of scales when computing scalograms and performing spectral analysis. The wavelet energy was estimated as

$$E(f,b) = |W(f,b)|^2. \qquad (3)$$

It can be interpreted as a local energy spectrum. Averaging of the energy $E(f,b)$ over the translation parameter $b$ provides the global energy spectrum $E(f)$, i.e., the scalogram.

Spectral energy was studied in two distinct frequency intervals:

I: 0.05–0.1 Hz. It is assumed that this interval is associated with rhythmic activity that has a metabolic origin. The corresponding activity may also be caused by the NO-related endothelial function.[22]

II: 0.1–0.3 Hz. This activity is associated with the neurogenic regulation and partial autonomic control.[23] Some studies also discussed the effects of metabolic activity in this frequency range.[24]

Besides the indicated ranges, other frequency intervals and regulatory mechanisms are considered.[22] According to the physiological assumptions we expect, however, possible changes in the CVBF-dynamics related to slow (and very slow) regulatory mechanisms, i.e., reflected in the indicated ranges I and II. Due to this, the given ranges were considered in detail in this work.

### 2.4. *Complexity measure*

Complexity analysis was performed with the wavelet-based multifractal formalism[25,26] that provides sensitive characteristics of signals structure in the case of highly inhomogeneous and nonstationary processes. Application of this tool in medicine allowed proposing the effective characteristics of heart failure.[27,28] Characterizing complexity with the wavelet-transform modulus maxima (WTMM)

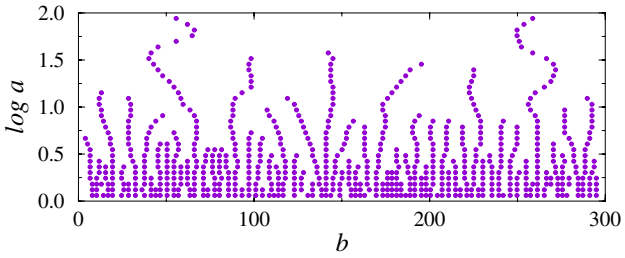


Fig. 2. Skeleton estimated with the continuous wavelet-transform using the MHAT-function.

method is based on the number of scaling characteristics that are required to describe the signal's features, i.e., on the multifractality degree. Simple processes such as $1/f$-noise are related to monofractal objects described by a single Hölder exponent $h$.[26] Physiological processes are typically characterized by a spectrum of Hölder exponents,[27,28] and the difference $\Delta = h_{\max} - h_{\min}$ can serve as a complexity measure of experimental data.

Estimation of this spectrum within the WTMM method is provided based on the partition functions constructed from wavelet coefficients. Unlike the function (2), real-valued wavelets are typically used in such estimations because the obtained results do not depend on $\psi$. Traditionally, multifractal analysis[25,26] is performed based on wavelets constructed as derivatives of the Gaussian function such as the Mexican hat (MHAT)-wavelet being its second derivative

$$\psi = (1 - \tau^2) \exp\left(-\frac{\tau^2}{2}\right). \tag{4}$$

Although analysis of frequencies is the traditional way in spectral applications, studies of multifractal measures with the wavelet-transform are based on scales. When computing wavelet-coefficients $W(a, b)$, lines of local minima and maxima of $W(a, b)$ are extracted at each fixed time scale $a$. The corresponding lines (called as the skeleton) contain main information about the wavelet-transform; they are used to compute the partition functions[26]

$$Z(q, a) = \sum_{l \in L(a)} |W(a, b_l(a))|^q \sim a^{\tau(q)}. \tag{5}$$

Here, $L(a)$ represents a full set of the skeleton's lines that can be detected at the scale $a$ (Fig. 2). At each scale $a$, the value of $b$ associated with the $l$th line is denoted as $b_l(a)$. The parameter $q$ characterizes local singularities at small ($q < 0$) and large ($q > 0$) scales.

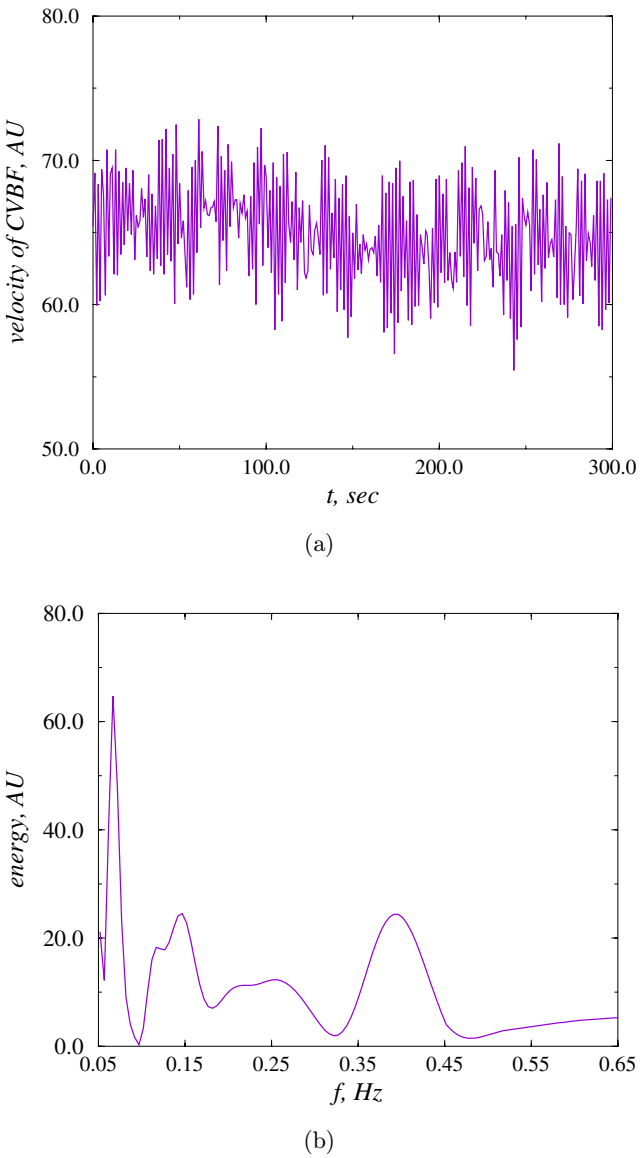


Fig. 3. Analyzed time series (a) and the scalogram (b).

Scaling exponents $\tau(q)$ estimated from the power-law dependence (5) are used for computing the Hölder exponents $h(q) = d\tau(q)/dq$ and the singularity spectrum

$$D(h) = qh - \tau(q) \tag{6}$$

being one of the most informative characteristics of the analyzed dynamics. The considered complexity measure $\Delta$ corresponds to the width of the singularity spectrum $D(h)$.

Such approach is significantly more stable as compared with direct estimations of the Hölder exponents $h(q)$ from experimental data.

## 3. Results and Discussion

### 3.1. *Spectral analysis*

Spectral analysis was performed for experimental data of CVBF-velocity for all three groups of animals. Examples of the analyzed data and the corresponding scalogram are shown in Fig. 3. Rhythmic components in both frequency intervals I and II are clearly detected. Besides, the scalogram contains additional peak related to the respiration.

Total spectral energy within the intervals I and II was estimated. According to Fig. 4, a reduced energy is observed in newborn rats with the developed ICH (24 h after the stress-off) as compared with the control group (I: $3.11 \pm 1.38$ vs $5.92 \pm 1.44$; II: $8.85 \pm 4.18$ vs $13.19 \pm 3.02$).

However, these distinctions are relatively small at the hidden stage of ICH (4 h after the stress-off) and the spectral energy cannot be considered as an appropriate measure of impairments of CVBF during the latent period of the development of ICH (I: $4.58 \pm 1.77$ vs $5.92 \pm 1.44$; II: $11.76 \pm 4.23$ vs $13.19 \pm 3.02$). The between-groups distinctions are not significant according to the Mann–Whitney test ($p > 0.05$).

### 3.2. *Complexity of CVBF*

Complexity of CVBF-velocity data was studied with the MTMM-method assuming that linear segments of the dependence $\log Z(q, a)$ vs $\log\ a$ are analyzed. In order to do this, too short skeleton's lines associated with oscillating "tails" of the wavelet-function (4) as well as fragments of the largest lines related to large values of $a$ (the latter can lead to essential errors due to a poor statistics) were excluded from the consideration.

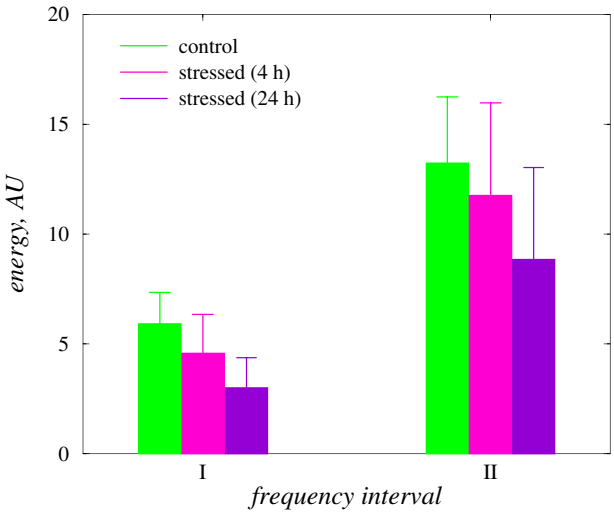


Fig. 4. Spectral energy estimated in two frequency intervals (mean ± SE).

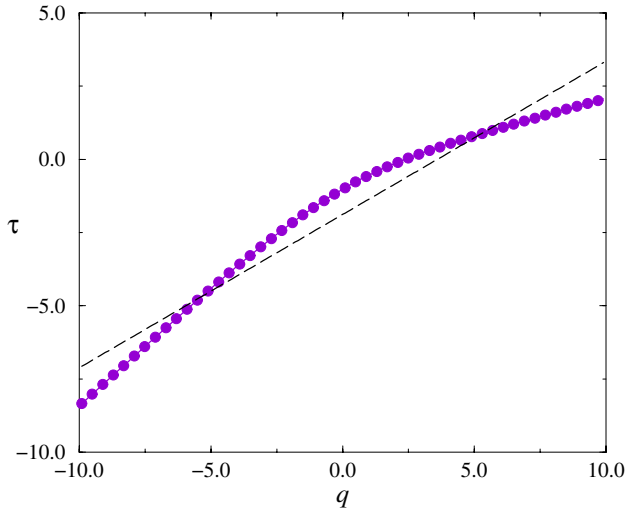


Fig. 5. Typical spectrum of scaling exponents showing a nonlinear dependence $\tau(q)$.

For all groups of animals, the dependence of scaling exponent from the parameter $q$ was clearly different from the linear function (Fig. 5) thus verifying that the analyzed data series possess multifractal properties and require large numbers of quantities to describe their scaling features.

The development of ICH was mainly associated with a reduced complexity of data series that was quantified by the measure $\Delta$. Figure 6 illustrates

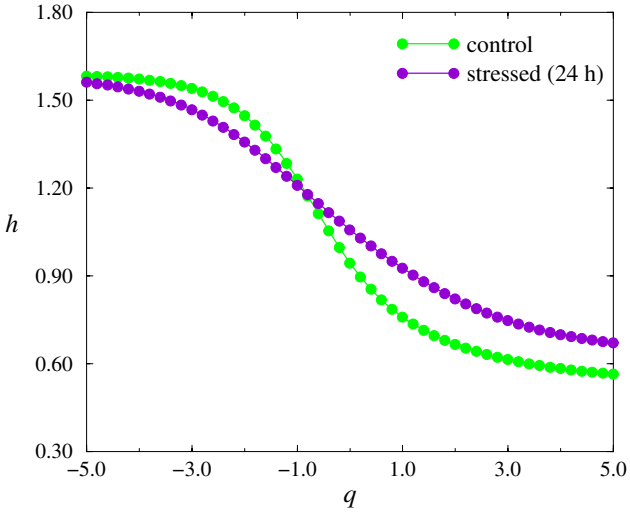


Fig. 6. Spectra of the Hölder exponents showing a reduction of complexity of CVBF-dynamics in a rat with ICH compared with a healthy animal.

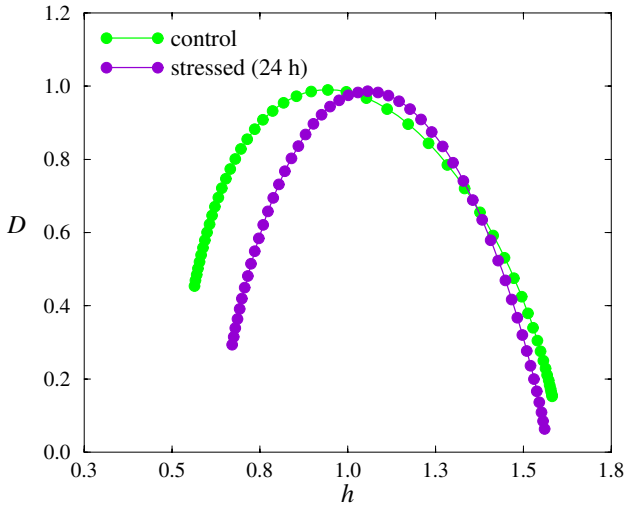


Fig. 7. Singularity spectra characterizing dynamics of CVBF in a healthy newborn rat and in a newborn rat with the stress-induced ICH.

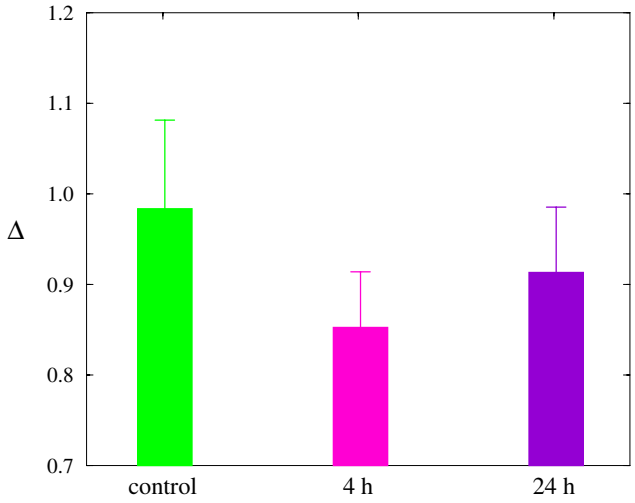


Fig. 8. Statistical analysis of the complexity measure Δ of CVBF-dynamics for three groups of animals (mean ± SE).

the spectra of Hölder exponents for a rat from the control group and from the group with the developed ICH. It is clearly seen that the difference between the maximal and minimal values of $h(q)$ reduces for pathological dynamics of CVBF.

In Fig. 7, the latter effect is illustrated using the singularity spectra. The narrower function $D(h)$ means a simpler dynamics of CVBF. Besides the reduction of the width of $D(h)$, a translation of the singularity spectrum along the $h$-axis may occur that reflects changed correlation properties of data series. However, this phenomenon is not essential for the macroscopic dynamics of CVBF in the sagittal sinus and, therefore, will not be considered further.

Statistical analysis performed for three groups of newborn rats verified a reduction of complexity measure Δ in animals with impairments of CVBF. Unlike the results of spectral analysis illustrated in Fig. 4, this reduction is distinguished at the hidden stage of the ICH development (4 h after the stress-off) — Fig. 8. Larger distinctions between the complexity measure Δ estimated for the control group and the group of stressed rats with the hidden stage of ICH (as compared with distinctions between the complexity measure computed for the control group and the group of stressed rats with ICH) may be caused by higher nonstationarity of CVBF data that is reflected in the scaling characteristics. Nevertheless, we can conclude that a reduced complexity of CVBF dynamics may serve as a marker characterizing an increased risk for ICH.

## 4. Conclusions

In this paper, we investigated the cerebrovascular dynamics in newborn rats based on LSCI and wavelet-analysis of the CVBF velocity aiming to reveal markers of early stages of the transformation of normal physiological processes into the pathological dynamics. We considered two wavelet-based approaches to characterize the spectral energy in distinct frequency intervals and complexity of CVBF.

Analysis of scalograms did not allow separation between the control group and the group of newborn animals with the hidden stage of ICH. Due to this circumstance, application of spectral analysis did not allow proposing prognostic criteria for a high risk of the development of ICH in newborns.

Complexity measure quantifying the width of the singularity spectrum represents a more sensitive characteristic of the hidden stage of ICH. Based on this measure, a reduction of complexity was revealed. The latter can be treated as a marker of pathological changes in CVBF. Unlike many other approaches, an advantage of the measure Δ is the possibility to quantify CVBF even for high nonstationarity and short data series. This circumstance is of a high importance for application of the considered measure in neonatal medicine where

signals with time-varying characteristics are typically recorded. Note that LSCI of the sinus blood flow is not possible noninvasively in human subjects limiting translatability of the approach. Nevertheless, revealing signs of early stages of the ICH development is an important circumstance for elaboration of new diagnostic methods for neonatal medicine.

## Acknowledgment

This work was supported by the Russian Science Foundation (Agreement 14-15-00128).

## References

1. R. W. Leech, P. Kohnen, "Subependymal and intraventricular hemorrhages in the newborn," *Am. J. Pathol.* **77**, 465–475 (1974).
2. J. Baun, "Neonatal intracranial hemorrhage," *J. Diagnostic Med. Sonography* **7**, 121–131 (1991).
3. P. Ballabh, A. Braun, M. Nedergaard, "Anatomic analysis of blood vessels in germinal matrix, cerebral cortex, and white matter in developing infants," *Pediatr. Res.* **56**, 117–124 (2004).
4. P. Ballabh, "Intraventricular hemorrhage in premature infants: Mechanism of disease," *Pediatr. Res.* **67**, 1–8 (2010).
5. J. D. Briers, S. Webster, "Laser speckle contrast analysis (LASCA): A non-scanning, full-field technique for monitoring capillary blood flow," *J. Biomed. Opt.* **1**, 174–179 (1996).
6. D. A. Boas, A. K. Dunn, "Laser speckle contrast imaging in biomedical optics," *J. Biomed. Opt.* **15**, 011109 (2010).
7. S. Liu, P. Li, Q. Luo, "Fast blood flow visualization of high-resolution laser speckle imaging data using graphics processing unit," *Opt. Express* **16**, 14321 (2008).
8. Y. Meyer, *Wavelets: Algorithms and Applications*, S.I.A.M., Philadelphia (1993).
9. Y. Meyer, *Wavelets and Operators*, Cambridge University Press, Cambridge (1993).
10. S. G. Mallat, *A Wavelet Tour of Signal Processing*, Academic Press, New York (1998).
11. P. S. Addison, *The Illustrated Wavelet Transform Handbook: Introduction Theory and Applications in Science, Engineering, Medicine and Finance*, IOP Publishing, Bristol (2002).
12. A. N. Pavlov, V. A. Makarov, E. Mosekilde, O. V. Sosnovtseva, "Application of wavelet-based tools to study the dynamics of biological processes," *Briefings Bioinformatics* **7**(4), 375–389 (2006).
13. A. N. Pavlov, V. S. Anishchenko, "Multifractal analysis of complex signals," *Phys. Uspekhi* **50**, 819–834 (2007).
14. A. N. Pavlov, O. N. Pavlova, "Analysis of correlation properties of random processes using short signals," *Tech. Phys. Letters* **34**, 306–308 (2008).
15. A. N. Pavlov, A. R. Ziganshin, O. A. Klimova, "Multifractal characterization of blood pressure dynamics: Stress-induced phenomena," *Chaos, Solitons Fractals* **24**, 57–63 (2005).
16. A. N. Pavlov, O. V. Sosnovtseva, O. N. Pavlova, E. Mosekilde, N.-H. Holstein-Rathlou, "Rhythmic components in renal autoregulation: Nonlinear modulation phenomena," *Chaos Solitons Fractals* **41**, 930–938 (2009).
17. A. N. Pavlov, O. N. Pavlova, E. Mosekilde, O. V. Sosnovtseva, "Characterization of renal blood flow regulation based on wavelet coefficients," *Fluct. Noise Lett.* **9**, 259–270 (2010).
18. O. V. Semyachkina-Glushkovskaya, V. V. Lychagov, O. A. Bibikova, I. A. Semyachkin-Glushkovskiy, S. S. Sindeev, E. M. Zinchenko, M. M. Kassim, H. A. Braun, F. Al-Fatle, L. A. Hassani, V. V. Tuchin, "The experimental study of stress-related pathological changes in cerebral venous blood flow in newborn rats assessed by DOCT," *J. Innov. Opt. Health Sci.* **6**(3) 1350023 (2013).
19. A. N. Pavlov, A. I. Nazimov, O. N. Pavlova, V. V. Lychagov, V. V. Tuchin, O. A. Bibikova, S. S. Sindeev, O. V. Semyachkina-Glushkovskaya, "Wavelet-based analysis of cerebrovascular dynamics in newborn rats with intracranial hemorrhages," *J. Innov. Opt. Health Sci.* **7**(1), 1350055 (2014).
20. A. N. Pavlov, O. V. Semyachkina-Glushkovskaya, Y. Zhang, O. A. Bibikova, O. N. Pavlova, Q. Huang, D. Zhu, P. Li, V. V. Tuchin and Q. Luo, "Multiresolution analysis of pathological changes in cerebral venous dynamics in newborn mice with intracranial hemorrhage: Adrenorelated vasorelaxation," *Physiol. Meas.* **35**, 1983–1999 (2014).
21. S. J. Kirkpatrick, D. D. Duncan and E. M. Wells-Gray, "Detrimental effects of speckle-pixel size matching in laser speckle contrast imaging," *Opt. Lett.* **33**, 2886–2888 (2008).
22. A. Stefanovska, M. Bračič, H. D. Kvernmo, "Wavelet analysis of oscillations in the peripheral blood circulation measured by laser Doppler technique," *IEEE Trans. Biomed. Eng.* **46**, 1230–1239 (1999).
23. R. Zhang, J. H. Zuckerman, K. Iwasaki, T. E. Wilson, C. G. Grandall, B. D. Levine, "Autonomic neural control od dynamic cerebral autoregulation in humans," *Circulation* **106**, 1814–1820 (2002).

24. R. I. Kitney, T. Fulton, A. H. McDonald, D. A. Linkens, "Transient interactions between blood pressure, respiration and heart rate in man," *J. Biomed. Eng.* **7**, 217–224 (1985).
25. J. F. Muzy, E. Bacry, A. Arneodo, "Wavelets and multifractal formalism for singular signals: Application to turbulence data," *Phys. Rev. Lett.* **67**, 3515–3518 (1991).
26. J. F. Muzy, E. Bacry, A. Arneodo, "The multifractal formalism revisited with wavelets," *Int. J. Bifurcation Chaos* **4**(2), 245–302 (1994).
27. P. Ch. Ivanov, L. A. Nunes Amaral, A. L. Goldberger, S. Havlin, M. G. Rosenblum, Z. R. Struzik, H. E. Stanley, "Multifractality in human heartbeat dynamics," *Nature* **399**, 461–465 (1999).
28. H. E. Stanley, L. A. Nunes Amaral, A. L. Goldberger, S. Havlin, P. Ch. Ivanov, C.-K. Peng, "Statistical physics and physiology: Monofractal and multifractal approaches," *Physica A* **270**, 309–324 (1999).